

Proof-of-Concept Static Thermomagnetic Generator Experimental Device

THEO CHRISTIAANSE and EKKES BRÜCK

A thermomagnetic power conversion device is constructed using water flows with very low caloric energy. The device has two active regenerators built from $(\text{Mn,Fe})_2(\text{P,As})$ materials suspended in a magnetic circuit as proposed by Brillouin and Iskenderian. The final magnetic circuit design was further optimized with finite-element simulations. The permanent magnet acting as field source was 1.4 kg of NdFeB alloy. The active part of the generator consists of 48 disks of $(\text{Mn,Fe})_2(\text{P,As})$ material with four different Curie temperatures of 300 K, 304 K, 307 K, and 310 K (27 °C, 31 °C, 34 °C, and 37 °C) measured in 1 T. Into each plate, micro-channels are laser cut. By stacking these plates in series, two regenerators with a gradient temperature span are built. Both regenerators have an exact weight of 26.9 g. The material was cycled at different speeds to find the maximum power output at the optimum frequency. Critical to a better design is a more tapered design and different materials. The tapered design ensures a greater external field and a larger external field change across the material. The materials for devices that use water as heat-transfer fluid in combination with this type of regenerator design should have a lower latent heat while maintaining their magnetic properties. This will increase the cycling speed and improve the power output of this type of device.

DOI: 10.1007/s40553-014-0006-9

© The Minerals, Metals & Materials Society and ASM International 2014

I. INTRODUCTION

SINCE the patents by Edison^[1] and Tesla^[2] in the late nineteenth century, there has been sporadic interest in the thermomagnetic generator (TMG). Halfway through the twentieth century, Brillouin calculated a high 55.5 pct Carnot efficiency for these types of devices. Thirty-six years after the paper of Brillouin and Iskenderian,^[3] Kirol and Mills^[4] published an even higher Carnot efficiency of 75 pct in a high external field device. This would be a huge improvement in efficiency compared to currently available technology; however, these efficiencies were generated with hypothetical materials properties that were not found in real materials at relevant temperatures. Recently, more interest has been generated by the development of magnetocaloric materials.^[5] These materials allow for the tuning of the Curie temperature by changing the chemistry of the active material.^[6] A recent paper by Vuarnoz *et al.*^[7] showed that this type of devices can be competitive with Organic Rankine Cycle devices when the energy source is waste heat. The engineering of this kind of devices is seldom reported in the literature.

A paper by Srivastava showed a thermomagnetic energy-conversion device using a permanent magnet. The active material is suspended above a permanent magnet and is pushed through its transition with a heat

gun. The material is heated and goes through a para-ferro-para-magnetic transition.^[8] This device has a low efficiency because it works between two different states. Well-established papers^[3,4,7] proposed the use of the regenerative Ericsson work cycle that theoretically could achieve much higher efficiencies in thermomagnetic energy-conversion devices.

In this work, a proof-of-concept experimental device is presented that works with a similar design as proposed by Brillouin and Iskenderian.^[3] We use $(\text{Mn,Fe})_2(\text{P,As})$ for the active magnetic material in the generator because the Curie temperature of this material can be tuned over a wide range around room temperature, and a small temperature change results in large changes in magnetization.^[9] The current device uses layered materials with different Curie temperatures to increase the temperature span. We structured the remainder of this article in four parts: First, the working principle is described, then the experimental design is elaborated. Experimental results are shown in Section IV. Because the device works on an alternating sequence, the optimum frequency of the device is found through a trial-and-error method. Finally, we discuss the results and give some suggestions for further research.

II. THE WORKING PRINCIPLE

The basic principle behind the TMG is to properly exploit the Faraday law across thermally induced magnetic phase transitions. The active materials used for this prototype have a typical ferromagnetic (FM)

THEO CHRISTIAANSE, Graduate Student, and EKKES BRÜCK, Professor, are with the Fundamental Aspects of Materials and Energy, Department of Radiation Science and Technology, Faculty of Applied Sciences, TU Delft, Mekelweg 15, 2629 JB Delft, The Netherlands. Contact e-mail: e.h.bruck@tudelft.nl

Manuscript submitted November 4, 2013.

Article published online January 22, 2014

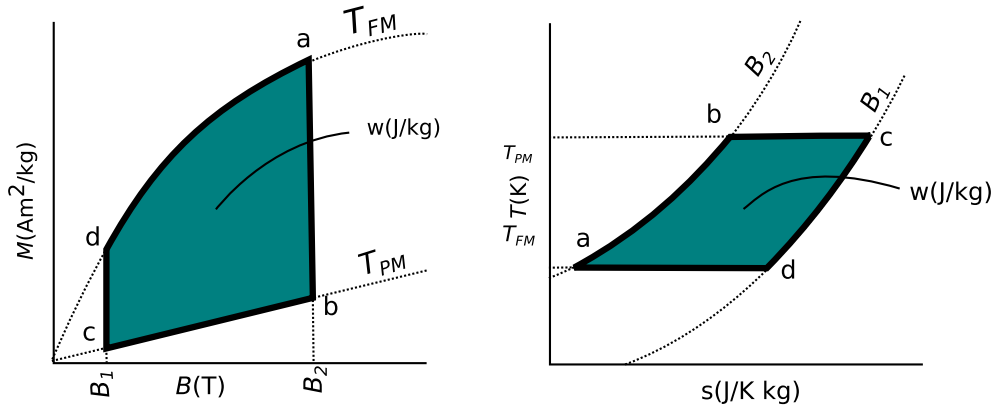


Fig. 1—Idealized work cycle for a thermomagnetic generator (TMG).

temperature profile. Here, the material is FM at low temperatures and becomes paramagnetic (PM) after crossing the Curie temperature (T_c).

Because cycling between just two states gives a very low efficiency,^[8] many researchers propose to use the regenerative Ericsson cycle.^[3,4,7,10,11] This cycle consists of two isothermal curves and two isofield curves. Graphically, this can be represented in two ways—either with a T - s diagram^[7,12] or via a M - B diagram^[3,13] (see Figure 1), where M is specific magnetization in Am^2/kg , B is the external field in T, s is the specific entropy in J/Kkg , T is in K ($^\circ\text{C}$), and w is the work done per kg material per cycle.

The material starts its work cycle (Figure 1) in a strong magnetic field B_2 at a temperature T_{FM} (point a). Heat is then added to the system until it warms up to T_{PM} . During the isofield process, the magnetization of the system decreases (from point a to b). Now the external field is lowered to B_1 (from point b to c), after which the temperature is restored to T_{FM} by cooling the system (from point c to d). By reapplying the field to B_2 , the magnetization is restored to its original point (point a).

The equations for work (W) are derived from the integral across the cycle in either plot (Eq. [1]).^[10]

$$W = V \oint \mu_0 H \cdot dM(T, H) = \oint T dS, \quad [1]$$

where V is the volume in m^3 , H in A/m , M in A/m , and μ_0 in $\text{J}/(\text{A}^2 \cdot \text{m})$.

A. Layered Material

The magnetic phase transition of each different material moves through a specific temperature range. To increase the working temperature span (ΔT) while keeping the same external field change, multiple materials are used with different working domains. The efficiency of the device is increased because the rejected heat from stage one is forwarded to the second stage. By tuning the working domains to the available heat sources, a better match can be constructed (see Figure 2).

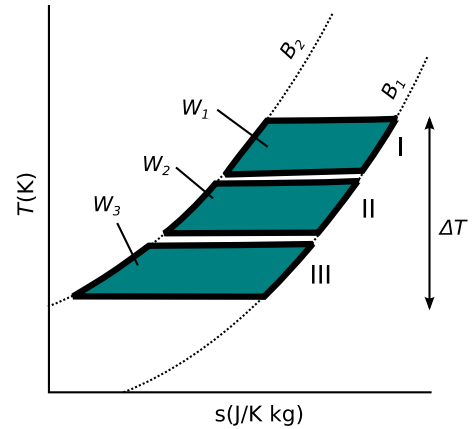


Fig. 2— T - s diagram of layered material.

III. EXPERIMENTAL DESIGN

The experimental design consists of two parts. The first part is the TMG itself. The second part includes auxiliary systems consisting of the water system and the electrical measurement and control system.

A. Thermomagnetic Generator

The TMG is constructed with one permanent magnet, two regenerators, and a magnetic circuit built from iron. The magnetic circuit has two purposes in the device. The first purpose is to direct the magnetic field from the permanent magnet to the regenerator. Second, when the magnetic permeability of the regenerator changes, the external field is directed to the higher permeability regenerator (Hopkinson's law). This causes the external field change needed for the work cycle.

1. Material

The $(\text{Mn,Fe})_2(\text{P,As})$ active material for this work was provided by BASF NL B.V. (Arnhem, NL). The material is called active because it actively contributes to the electricity production; 48 disks ($\varnothing_d = 18$ mm and 1.0 mm thick) of four different Curie temperatures were provided. In 1T, the T_c are 300 K, 304 K, 307 K, and

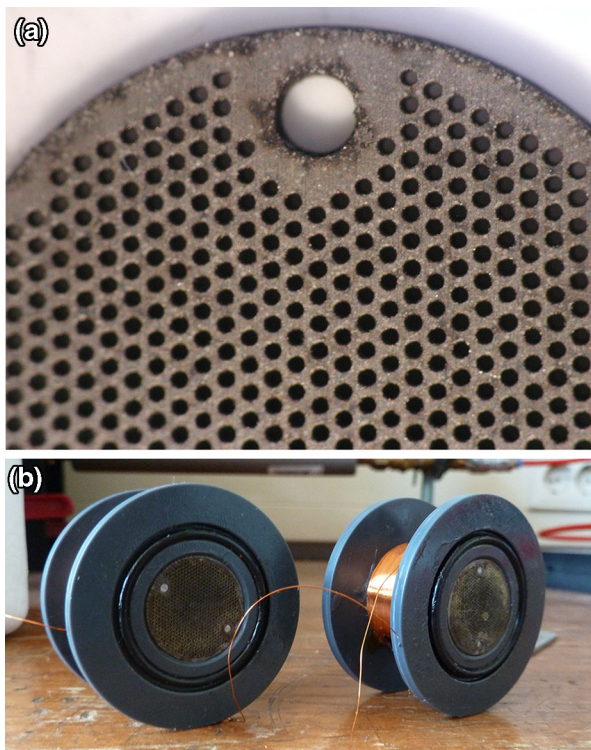


Fig. 3—(a) MnFe(P,As) plate, provided from BASF and (b) finalized regenerators.

310 K (27 °C, 31 °C, 34 °C, and 37 °C). On the surface of the plates, small holes ($\varnothing_h = 300 \mu\text{m}$) were laser cut. To construct the regenerators, these plates are divided into two even stacks. The stacks are then bound together through two axes on either side of the plates (Figure 3). The total active material weight per regenerator is 26.9 g. The resulting microchanneling regenerator gives a high heat transfer coefficient and material density compared to the plate heat exchanger designs. These advantages were, however, not realized in this study, as it turned out that due to the laser cutting, 60 wt pct of the remaining material became inactive. This weight percentage is calculated from the theoretical magnetization vs the measured magnetization of the material in the device. To construct the finalized regenerators, the regenerator was placed into a retainer. Each retainer was provided with a pickup coil of 240 turns and an O-ring to provide the water seal. The number of turns was determined from the theoretical magnetization of the material and resolution of the voltmeter.

2. Magnetic circuit

By using the computer package Radia (European Synchrotron Radiation Facility, ESRF, Grenoble, France), a finite-element plug-in running on Mathematica (Wolfram Research, Champaign, IL), a first design based on the Brillouin static generator was constructed and optimized for the maximum change in magnetic field (see Figure 4).^[14,15] As input for the simulations, we used measured values of the field generated by a NdFeB magnet, magnetically soft pure Fe, and the

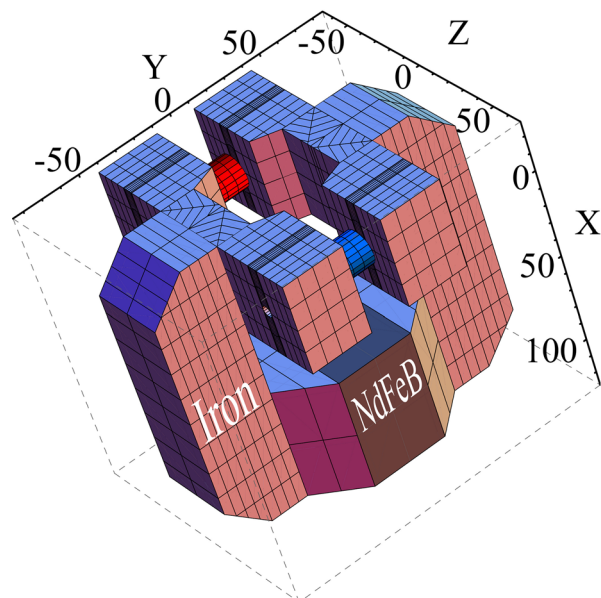


Fig. 4—Three-dimensional graphic made in Mathematica, PM state magnetocaloric material in red, and FM state magnetocaloric material in blue (Color figure online).

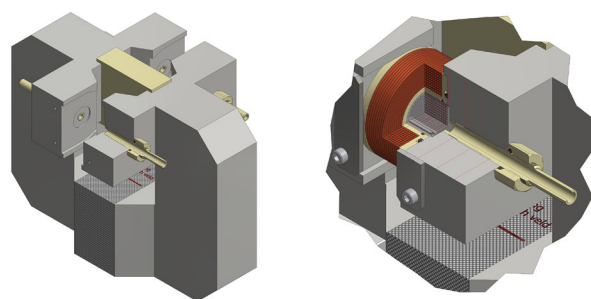


Fig. 5—Final design of the magnetic circuit made in AutoCAD.

magnetic response of $(\text{Mn,Fe})_2(\text{P,As})$ materials that were used to make the plates. The mean external field calculated by Radia for our design is 0.21 T and the field change during the two isothermal processes is 0.08 T.

3. Final design

From this preliminary design, a practical design was drawn in AutoCAD (Autodesk, Inc., San Rafael, CA) considering three constraints. First, there was only a limited amount of active material custom made for this device. This set the gap length between the two pole faces. Second, the NdFeB magnet had a weight of 1.4 kg and strength of $1.15 \pm 0.05 \text{ T}$. Third, a water seal was implemented between the pole face and the regenerator. The final design constructed is shown in Figure 5. The mean external field measured between the two pole faces was measured at 0.24 T and the change 0.01 T.

B. Auxiliary System

To provide the water flow for the thermal cycling, a one-way water system (not a closed cycle) was built

(Figure 6). Two water barrels were pressurized by air to provide the water pressure. Both barrels are filled with water at room temperature; for the hot flow, an extra heat exchanger is added. By measuring the temperature at the experimental setup and regulating this heat exchanger, the temperature of the water flow was kept constant. The water was then directed to the two different regenerators by four computer-controlled three-way valves. The computer is used to provide the timing of the system so the regenerators are cycled cooperatively to change the external field. The water is then passed to a capture tank. After each experiment, the water is properly discarded after purification as it may be contaminated with As.

For the computer setup, Labview (National Instruments, Austin, TX) is used to quickly build the hardware–software interface and automate the experiments. The computer setup has three distinct crucial functions for the experiment. First, to maintain experimental water temperature conditions during the experiments, the temperature is measured. The computer program registers the temperature of the ingoing and outgoing flows with four *J*-type thermocouples. The thermocouples are readout by a four-channel thermocouple interface board (National Instruments (NI9211).

Second, to calculate the power output of the device, the voltage across the coils is measured. To measure the voltage from the coils, a Keithley (Keithley Instruments, Solon, OH) 2100 Nanovolt meter is used. The Keithley has a USB interface with the computer, and we used the official software provided by Keithley for Labview.

Third, to control the valve switching for the experiments, four 3-way valves are used from Fluid Automation Systems (CH-1290; Versoix, Switzerland). These valves allow for a quick simultaneous switching. To quickly activate the valves, Labview uses a USB interfaced microcontroller board (Arduino; open-source electronics prototyping platform) and LIFA software (Labview Interface For Arduino).

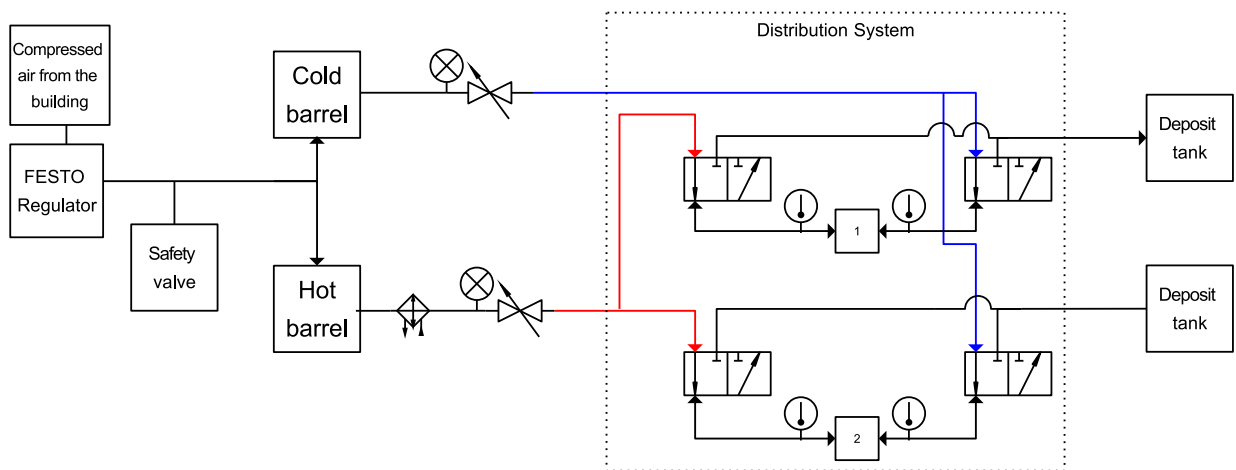


Fig. 6—Schematic drawing of the water auxiliary system.

IV. RESULTS

As one of the regenerators is cooled, the other is heated. This allows for the regenerators to work in cooperation to change the external field as much as possible. A full cycle is defined as the heating and cooling of one regenerator. The heating and cooling is done by the hot and cold water flows, respectively. For example, see Figure 7; the whole cycle takes 10 seconds. In 5 seconds, the regenerator 1 is cooled and regenerator 2 is heated, then after 5 seconds the regenerator 1 is heated and regenerator 2 is cooled. The flux change in the materials causes an induced voltage in the coils wrapped around the material. The compounded voltage from the coils was measured with a Keithley 2100 nanovolt meter integration time set to 0.05 second. The data from the nanovolt meter were read each 0.10 second.

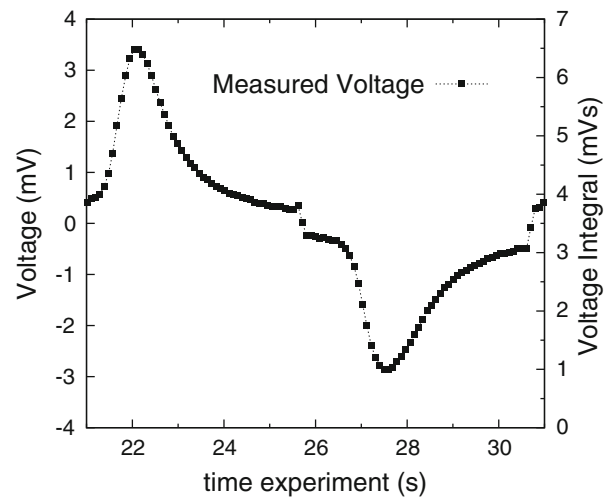


Fig. 7—Voltage drop registered from a 10 s period cycle (lines are given to guide to the eye).

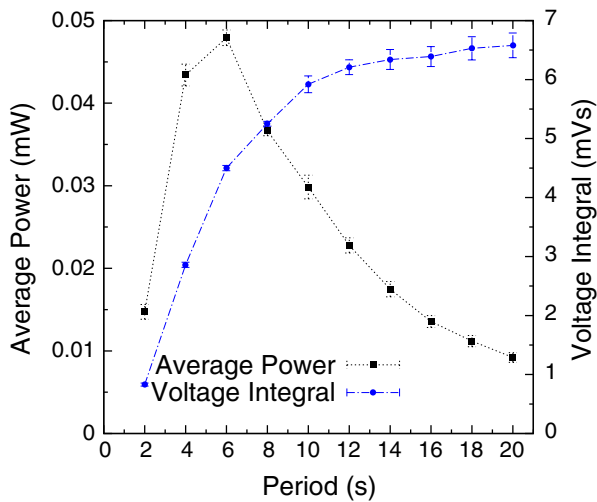


Fig. 8—Frequency dependence of the power output (lines are given to guide to the eye).

The power was calculated from the average voltage measured and the internal resistance ($R_i = 23.51 \Omega$) (Eq. [2]). The average voltage was calculated from the area under the voltage curve measured each half cycle (Eq. [3])

$$W_e = \frac{V_{ave}^2}{2R_i} \quad [2]$$

$$V_{ave} = \frac{1}{t_2 - t_1} \int_{t_1}^{t_2=1/2p+t_1} |V(t)| dt. \quad [3]$$

By measuring the voltage curve across five cycles, at each cycle speed, with a fixed temperature span of $(17 \text{ to } 33) \pm (1 \text{ }^\circ\text{C})$, the average power could be determined through the voltage integral. The results from this set of experiments are displayed in Figure 8.

The power output reaches its maximum at a 6-seconds period speed or 0.17 Hz. After this point, the power drops off because not enough heat is transferred to the regenerator to cycle the material through the magnetic phase transition. This rather poor cycling behavior is attributed mainly to the degradation of magnetic properties caused by the laser treatment. Essentially, the walls of the water channels were transformed into magnetically inactive material that only poses a thermal resistance and heat capacity.

V. CONCLUSION AND DISCUSSION

First, the magnetic circuit was not effective enough in changing the external field. The Radia simulation gave an external field change of 0.08 T . A measurement done on the magnetic circuit gave an external field change of about 0.01 T . This reduced external field change is due to the fact that most of the active material was

compromised during laser treatment. As only a small fraction of the material is changing from PM to FM, the magnetic circuit hardly changes. This also results in the strongly reduced filling factor of the coil. The combination of these two effects gave a very low electrical work output, which in comparison with the simulations was reduced by a factor of 800.

To get high power output, heat transfer properties of the material become essential. Limited thermal conductivity can be compensated for by properly structuring the flow channels. Another route to gain output power is decreasing the specific heat of the material across the transition, as then the transition would run faster and the power is increased. This indicates that materials that operate optimal for heat pumps may not be the best choice for magnetocaloric power generation. Second, the morphology of these materials for use in these designs needs more research. The $(\text{Mn,Fe})_2(\text{P,As})$ material was nearly completely compromised due to the laser treatment. The improvement of this method or other means of shaping the regenerators should be explored.

ACKNOWLEDGMENT

This work is part of an Industrial Partnership Program of the Dutch foundation for Fundamental Research on Matter (FOM), co-financed by BASF New Business. We also would like to thank AK Steel, Magnet Physik, Bautou Research Institute of Rare Earths and Thermo Electra for providing materials, services, permanent magnet alloy and sensors, respectively.

REFERENCES

1. T.A. Edison: Patent No. 476983, 1892.
2. N. Tesla: Patent No. 428057, 1890.
3. L. Brillouin and H.P. Iskenderian: *Thermomagnetic Generator*, Federal Telecommunication Laboratories, Nutley, NJ, 1948, pp. 300–13.
4. L.D. Kirol and J.I. Mills: *J. Appl. Phys.*, 1984, vol. 56 (3), p. 824.
5. N.H. Dung, Z.Q. Ou, L. Caron, L. Zhang, D.T.C. Thanh, G.A. De Wijs, R.A. De Groot, K.H.J. Buschow, and E. Brück: *Adv. Energy Mater.*, 2011, vol. 1, pp. 1215–19.
6. G. Degen, B. Reesink, and E. Brueck: U.S. Patent 0037342, 2011.
7. D. Vuarnoz, A. Kitanovski, C. Gonin, Y. Borgeaud, M. Delessert, M. Meinen, and P.W. Egolf: *Appl. Energy*, 2012, vol. 100, pp. 229–37.
8. V. Srivastava, Y. Song, K. Bhatti, and R.D. James: *Adv. Energy Mater.*, 2011, vol. 1 (1), pp. 97–104.
9. O. Tegus, E. Brück, K.H.J. Buschow, and F.R. de Boer: *Nature*, 2002, vol. 415 (6868), pp. 150–52.
10. A. Kitanovski and P.W. Egolf: *Int. J. Refrig.*, 2006, vol. 29 (1), pp. 3–21.
11. D. Solomon: *J. Appl. Phys.*, 1988, vol. 63 (3), p. 915.
12. D. Vuarnoz, A. Kitanovski, C. Gonin, and P.W. Egolf: *Int. J. Exergy*, 2012, vol. 10 (4), p. 365.
13. C.-J. Hsu, S.M. Sandoval, K.P. Wetzlar, and G.P. Carman: *J. Appl. Phys.*, 2011, vol. 110 (12), p. 123923.
14. P. Elleaume, J. Chavanne, and F.-G. Cedex: *ESRF*, 1997, pp. 3509–11.
15. A. Smirnov, D. Newsham, Y. Luo, D. Yu, G. Biillas, R. Wines, and N. News: *Particle Accelerator Conference SHORT*, 2003, pp. 2135–37.